A&A 392, 1081–1088 (2002)
DOI: 10.1051/0004-6361:20020981

Astronomy & Astrophysics

Photodissociation of CO in turbulent molecular clouds

M. Röllig[1], M. Hegmann, and W. H. Kegel

Institut für Theoretische Physik/Astrophysik, Johann Wolfgang Goethe-Universität, Robert-Mayer-Str. 8–10, 60325 Frankfurt a.M., Germany
e-mail: roellig@astro.uni-frankfurt.de

Received 22 April 2002 / Accepted 27 June 2002

Abstract. We study the formation of CO molecules at the edge of dense molecular clouds. As shown by van Dishoeck & Black 1988 the CO photodissociation process is dominated by line rather than continuous absorption. Hence, a turbulent velocity field, modifying the line shape, strongly affects the CO density distribution. We investigate these effects in detail. To describe the turbulent velocity field we use the statistical approach by G. Traving and collaborators (cf. Gail et al. 1974) which accounts for a finite correlation length for the velocity field. We solve the radiative transfer equation selfconsistently with the rate equations describing the chemical reactions. One main goal of the investigation is an improvement of molecular cloud models used to analyze observational data. To bring the observational data into agreement with the model of an isothermal spherical cloud being stabilized by turbulent and thermal pressure it turned out to be neccessary to implement a cut off radius for the CO density distribution in order to define a cloud edge (Piehler & Kegel 1995). This radius depends heavily on the intensity and density distribution in the outer parts of the cloud. Our calculations show that turbulence has substantial influence on the penetration of UV radiation into a molecular cloud. Even turbulent velocities in the order of a few thermal velocities are sufficient to allow the radiation to penetrate significantly deeper into the cloud than in a nonturbulent medium. On the other hand correlation length effects may lead to a decrease in photodissociation efficiency. By accounting for a finite correlation length of the stochastic velocity field the self-shielding of CO absorption bands is considerably enhanced and CO molecules can effectively form in depths that have a much stronger UV intensity in standard radiative transfer models.

Key words. radiative transfer – turbulence – ISM: clouds – ISM: molecules – ultraviolet: ISM – line: formation

1. Introduction

Shielded from far ultraviolet (FUV) radiation, the gas inside dense interstellar clouds occurs mainly in molecular form. On the surface of these clouds, FUV photons heavily effect the physical and chemical structure of the interstellar medium (ISM) by means of photoionization and photodissociation processes. One of the keys to understanding these photon-dominated regions (PDRs) lies in understanding the attenuation of the FUV flux through the PDR. Hence, various authors have studied the penetration of FUV radiation into molecular clouds. However, most of the early work was done for homogeneous clouds only (e.g. Roberge et al. 1991). In recent years, it has become increasingly clear that interstellar clouds are inhomogeneous down to the smallest accessible scales (see e.g. Falgarone & Phillips 1996). Authors, which studied the profound influence of this clumpy structure of interstellar clouds on the radiative transfer, are for example Boissé (1990), Hobson & Scheuer (1993), Spaans (1996), and Hegmann & Kegel (1996).

Send offprint requests to: M. Röllig,
e-mail: roellig@astro.uni-frankfurt.de

Most of these studies were done for the transport of radiation in the continuum. Hence, the influence of a turbulent velocity field on the radiative transfer was neglected in general. However, a turbulent velocity field becomes important, if, as in the case of CO, photodissociation takes place by line absorption into predissociated bound states rather than by continuous absorption (van Dishoeck & Black 1988). Since, in addition, line absorption by CO dominates over absorption and scattering by dust, the formation rate of CO is strongly subject to velocity fluctuations within the cloud.

The present paper is aimed at studying the effects of a turbulent velocity field on the formation of CO. The spatial variation of the turbulent velocity field is described in a statistical sense only. Following Gail et al. (1974), the variation of the turbulent velocity field along each line of sight is assumed to correspond to a Markov process. This approach accounts for a finite correlation length of the turbulent velocity field.

Our calculations show, that both, the mean square turbulent velocity and the correlation length, strongly affect the shape and the strength of the CO absorption lines (see e.g.: Levshakov & Kegel 1994). As a consequence, the CO abundance is modified, too. In particular it has turned out, that self-shielding of CO is considerably enhanced by accounting for

a finite correlation length ℓ of the turbulent velocity field. CO can be effectively formed in depths that would have a much stronger FUV intensity in conventional microturbulent models ($\ell \to 0$).

We accounted for a small chemical network consisting of 38 different species interacting in 434 reactions. As cloud geometry we assumed a plane parallel semi infinite slab. In this work we present calculations done for a uniform density distribution with constant gas temperature.

2. The model

2.1. Stochastic description of the velocity distribution

Here we give a short summary of our statistical approach only. For a detailed description of the model see Hegmann & Kegel (2000) and Gail et al. (1974) and references therein. The turbulent velocity field is described in a statistical sense only. We assume the one-point distribution function of the component of the hydrodynamical velocity along the line of sight to be given by a Gaussian

$$p(v) = \frac{1}{\sqrt{2\pi}} \exp\left(-\frac{v^2}{2\sigma^2}\right) \tag{1}$$

with σ being the mean square turbulent velocity. The two-point correlation function

$$f(\Delta s) = \frac{< v(s)v(s+\Delta s) >}{\sqrt{< v^2(s) >< v^2(s+\Delta s) >}} \tag{2}$$

we assume to be given by

$$f(\Delta s) = \exp\left(-\frac{\Delta s}{\ell}\right). \tag{3}$$

ℓ is the correlation length of the velocity fluctuations and has the physical meaning of a length scale for variations of v. The assumptions (1) and (3) are consistent with the assumption that the variation of v along each line of sight is governed by a Markov process.

2.2. The generalized radiative transfer equation

If the density and velocity distribution is known, the propagation of radiation inside a medium along a line of sight s can be calculated by means of the ordinary radiative transfer equation:

$$\frac{\mathrm{d}I_\nu}{\mathrm{d}s} = -\kappa_\nu(s) I_\nu(s) + \epsilon_\nu(s). \tag{4}$$

In interstellar clouds reemission of FUV photons is negligible. Due to this and for the sake of numerical simplicity we neglected scattering by dust. This is equal to the assumption of pure forward scattering and leads to the radiative transfer equation for pure absorption:

$$\frac{\mathrm{d}I_\nu}{\mathrm{d}s} = -\kappa_\nu(s) I_\nu(s). \tag{5}$$

Since the velocity distribution along the cloud is unknown, Eq. (5) cannot be solved directly. With the assumption of a stochastic velocity field the intensity has to be treated as a stochastic variable. (1), (3) and (5) lead to a generalized radiative transfer equation (Gail et al. 1974; Hegmann & Kegel 2000):

$$\frac{\partial q_\nu}{\partial s} = \frac{1}{\ell}\left(-v\frac{\partial q_\nu}{\partial v} + \sigma^2 \frac{\partial^2 q_\nu}{\partial v^2}\right) - \kappa_\nu q_\nu, \tag{6}$$

which has to be solved with the initial condition

$$q_\nu(v, s=0) = I_{\nu,0} \tag{7}$$

and the boundary conditions

$$\lim_{v\to\pm\infty} q_\nu(v, s) = I_{\nu,0}. \tag{8}$$

$q_\nu(v, s)$ is the conditional intensity and can be understood as the conditional expectation value of the intensity for a given velocity v at point s. The mean value for the intensity can be calculated from $q_\nu(v, s)$ by the quadrature:

$$\langle I_\nu(s)\rangle = \int_{-\infty}^{+\infty} q_\nu(v, s) p(v) \mathrm{d}v. \tag{9}$$

2.3. The absorption coefficient

The photodissociation of CO molecules is known to be dominated by line rather than continuous absorption. In the wavelength range 912 Å $\leq \lambda \leq$ 1118 Å no absorption continuum can be found (Letzelter et al. 1987). Instead, a great number of discrete absorption bands can be seen. It has been shown (Letzelter et al. 1987; Eidelsberg et al. 1991) that the photodissociation of CO occurs through absorption of photons in discrete rotational lines from the ground vibrational state towards excited predissociated Rydberg electronic states. Predissociated means, that these excited states overlap with the dissociative continuum of a lower state. Thus there is a finite probability of a radiationless transition to the lower unbound state. Together with the continuous absorption by dust the overall absorption coefficient can be written as:

$$\kappa_\nu = \kappa_{\mathrm{dust}} + \kappa_{\mathrm{CO}}, \tag{10}$$

with κ_{CO} beeing the absorption cross section $k_{v'J',0J''}$ times the CO number density n_{CO}:

$$\kappa_{\mathrm{CO}} = \kappa_{v',0}(\nu, v) = n_{\mathrm{CO}} \sum_{J''} \tilde{n}_{J''} \sum_{J'} k_{v'J',0J''}(\nu, v), \tag{11}$$

with the upper state $(v'J')$ and the lower state $(0, J'')$. $\tilde{n}_{J''}$ is the relative occupation number for the lower rotational state. We used the spectroscopic parameters from Warin et al. (1996). We account for a pure thermal occupation with an constant excitation temperature of 15 Kelvin up to a rotational quantum number of $J = 4$ even at much higher gas temperatures. This approximation is not too bad since Warin et al. (1996) showed that rotational level occupation is strongly underthermal. Therefore, and since the computational time heavily depends on the total number of lines we did not account for J'' states higher than 4. The absorption cross section per molecule is given by:

$$k_{v'J',0J''}(\nu, v) = \frac{\pi e^2}{m_{\mathrm{e}} c} f_{v'J',0J''} \Phi(\nu, v) \tag{12}$$

Table 1. List of all species included in the chemical network.

Included spezies						
H	He	C	O	H^+	He^+	C^+
O^+	e^-	H^-	C^-	O^-	H_2	O_2
H_2^+	O_2^+	CH	CO	OH	CH^+	CO^+
OH^+	OH^-	H_3^+	H_2O	H_2O^+	HCO	HCO^+
CH_2	CH_3	CH_4	CH_2^+	CH_3^+	CH_4^+	CH_5^+
H_3O^+	H_2CO	H_2CO^+				

f being the line oscillator strength and Φ the profile funtion. Under interstellar conditions the profile function $\Phi(\nu, v)$ is determined by thermal broadening and radiation damping, leading to a Voigt profile

$$\Phi(\Delta\nu) = V(\alpha, \mathrm{v}) = \frac{\alpha}{\Delta\nu_\mathrm{D}\pi^{\frac{3}{2}}} \int_{-\infty}^{+\infty} \frac{e^{-y^2}\mathrm{d}y}{\alpha^2 + (\mathrm{v} - y)^2} \tag{13}$$

with,

$$\alpha = \frac{\gamma}{4\pi\Delta\nu_\mathrm{D}} \text{ and } \mathrm{v} = \frac{\Delta\nu}{\Delta\nu_\mathrm{D}}. \tag{14}$$

γ is the inverse lifetime of the upper level and $\Delta\nu = \nu - \nu_0$. For the dust absorption we adopted an absorption coefficient given by Tielens & Hollenbach (1985):

$$\kappa_\mathrm{dust} = n_\mathrm{dust}\sigma_\mathrm{dust} = 5 \times 10^{-22} n\, \delta_\mathrm{uv}\delta_\mathrm{d} \tag{15}$$

with $\delta_\mathrm{uv} = 1.8$, $\delta_\mathrm{d} = 1.0$, and the hydrogen nucleus number density n.

2.4. The rate equation

We assume chemical equilibrium and determine the relative abundances from a chemical network consisting of 38 different species formed and destroyed in 434 reactions (Millar et al. 1995; Le Teuff et al. 2000). All processes forming and destroying a specific species i are described in the rate equations:

$$n_i \left\{ \tilde{\zeta}_i + \sum_q n_q k_{qi} \right\} = \sum_r \sum_s k_{rs} n_r n_s + \sum_t n_t \tilde{\zeta}_{ti}, \tag{16}$$

with the densities n_q, n_r, n_s of all species participating in chemical reactions forming or destroying i. The left hand side of Eq. (16) represents all destruction processes, the right hand side represents all formation processes. $\tilde{\zeta}$ accounts for photodissociation ζ^diss and photoionisation ζ^ion. $\tilde{\zeta}_i$ covers all photodestructive reactions of i while $\tilde{\zeta}_{ti}$ is the rate coefficient for the photodestruction of t leading to the formation of i.

2.5. Hydrogen

Hydrogen plays a key role in both parts of our model: Firstly, H_2 is a very strong absorber for UV photons penetrating the cloud and due to its broad absorption lines is very effective in shielding deeper parts from photodestruction. This affects the CO absorption spectrum as well. There is a significant number of CO absorption bands that are at least partially overlapped by broad hydrogen absorption lines. In order to save computing time, we considered all CO absorption bands overlapping with hydrogen lines to be completely shielded. This is the case for the bands: 7D, 9A, 13, 14, 15A, 15B, 19, 24, 31, 33, 38 (we applied the identification scheme and spectroscopic parameters from Warin et al. 1996).

Secondly, it is an important part for the chemical evolution of the cloud. The formation of H_2 takes place on the surface of interstellar dust grains:

$$\mathrm{H} + \mathrm{H} + \text{ dust} \rightarrow \mathrm{H_2} + \text{ dust} \tag{17}$$

with the reaction rate $Rnn_\mathrm{H}\,(\mathrm{s^{-1}\,cm^{-3}})$. Here n is the total hydrogen particle density ($n = n_\mathrm{H} + 2n_{\mathrm{H_2}}$) and n_H the atomic hydrogen density (Sternberg & Dalgarno 1995). R is the H_2-formation rate coefficient:

$$R = 3 \times 10^{-18} f_a S\, T^{1/2}\ \mathrm{cm^3\ s^{-1}}. \tag{18}$$

Here T is the gas temperature, S is the gas-grain sticking coefficient, and f_a the fraction of hydrogen atoms that are available for molecule formation. From Burke & Hollenbach (1983) and Hollenbach & McKee (1979) we find:

$$S = [1 + 0.04(T + T_\mathrm{dust})^{1/2} + 2 \times 10^{-3} T + 8 \times 10^{-6} T^2]^{-1}, \tag{19}$$

and

$$f_\mathrm{a} = \frac{1}{1 + 10^4 \exp(-600/T_\mathrm{dust})}. \tag{20}$$

To account for the photodissociation properties of H_2 we took the hydrogen shielding factors $\Theta(H_2)$ given by Lee et al. (1996):

$$\zeta_{\mathrm{H_2}}(N(\mathrm{H_2}) = G_0 \times \zeta_{\mathrm{H_2}}(0) \times \Theta[N(\mathrm{H_2})], \tag{21}$$

with $N(H_2)$ being the hydrogen column density and G_0 an enhancement factor for the FUV field. The photodissociation rate coefficient for hydrogen at the edge of a cloud is:

$$\zeta_{\mathrm{H_2}}(0) = 2.54 \times 10^{-11}\ \mathrm{s^{-1}} \tag{22}$$

for an UV enhancement factor of $G_0 = 1$ and a standard UV field (Mezger et al. 1982).

In the present context we are mainly interested in the photodissociation of CO which we treat in considerable detail. In contrast to this, we model the photodissociation of H_2 only crudely using shielding factors (Lee et al. 1996). This appears justifiable since photodissociation of H_2 is important only in a rather shallow layer ($N \lesssim 10^{18}\ \mathrm{cm^{-2}}$). This implies that in most of the volume we are considering, hydrogen is found almost completely in the form of H_2. Furthermore, in greater depths the H_2 lines are dominated by their damping wings and therefore are almost independent of the details of the velocity field.

2.6. CO

The photodissociation is subject to different shielding effects (van Dishoeck & Black 1988):

1. Self shielding: the photodissociation rate of every single absorption line depends on the density and the intensity in the local frame of rest. At the edge of the cloud absorption

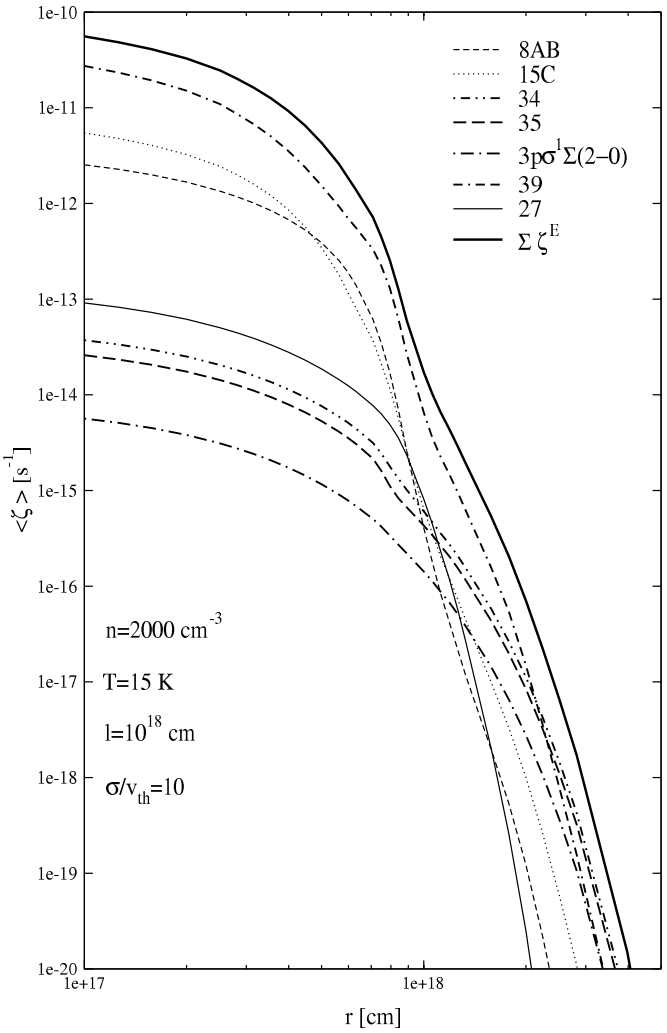

Fig. 1. Depth dependence of $< \zeta >$ for different absorption bands.

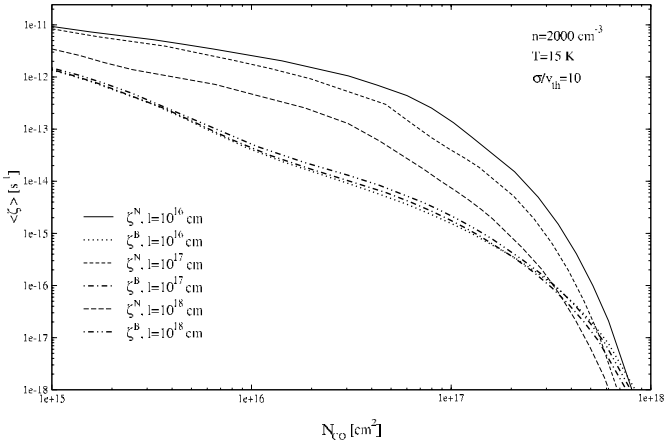

Fig. 2. Photodissociation rate coefficients of the broad bands ζ^{B} and narrow bands ζ^{N} for different correlation lengths.

bands with strong absorption lines dominate the total photodissociation rate. In deeper parts the line centers become optically thick and absorption takes place in the line wings. Absorption bands which dominate at the cloud edge may be of minor importance in greater depths. Figure 1 shows the contribution of different absorption bands to the expectation value of the total photodissociation rate coefficient of all "narrow" absorption bands.

2. Hydrogen shielding: as mentioned above, all CO absorption bands shielded by hydrogen are considered to be fully shielded from any UV photons and therefore are not considered in further line calculations.
3. Mutual shielding: absorption lines of the rarer isotopomers ^{13}CO and C^{18}O may overlap with corresponding bands of the main isotopomer. Many bands of all three species have almost identical line wavelengths. Warin et al. (1996) showed that mutual shielding is too weak to be of importance in calculating the dissociation rate of ^{12}C^{16}O. We did not consider mutual shielding effects in our calculations, since we restricted our investigation to ^{12}C^{16}O.
4. Shielding by dust.

2.7. Numerical aspects

The non-local coupling of the radiation field and the molecular abundances over the whole cloud is one of the main characteristics of our model. It is neccessary to simultaneously solve the radiative transfer Eq. (6) with the rate equation for all points in physical space and velocity space. We use the finite differences method of Cranck-Nicolson to solve the generalized radiative transfer equation together with numerical routines using a modified Powell Hybrid method to solve the system of rate equations. This is done in an iterative way: starting with a density distribution for all species the resulting radiation field is computed. Using the new radiation field we recalculated the densities. Then the next iteration step starts. In order to save computing time not all absorption bands are calculated by means of the generalized radiative transfer equation. Absorption bands with small radiative lifetimes are showing the strongest overlap of individual absorption lines. Radiative lifetimes in the order of $10^{-11} \ldots 10^{-12}$ s correspond to natural line widths of 2–20 km s^{-1} compared to turbulent velocities of a few km s^{-1}. These broad absorption bands would hardly respond to turbulent variations of their individual components. It is therefore a reasonable simplification to compute these bands in the microturbulent approximation. We divided the set of CO absorption bands in two groups:

- bands with well distinguishable narrow lines are computed with the generalized radiative transfer equation: 7A, 7BC, 8AB, 9B, 9C, 15C, 20, 25, 27, 28, $^3\Pi$(3–0), 34, 35, 36, 3p$\sigma^1\Sigma$(2–0), 37, 39;
- bands with very broad absorption features are calculated by means of the ordinary transfer equation: 10, 12, 16, $^1\Sigma$, 17, 18, 21, 22, 23, 26, 29, 30, 32, 3p$\sigma^1\Sigma$(4–0), 41.

As a result we receive two contributions to the total photodissociation rate coefficient ζ. Figure 2 shows the total photodissociation rate coefficient for narrow and broad bands calculated for different correlation lengths. Only for high CO column densities the broad bands contribute significantly to the total rate coefficient.

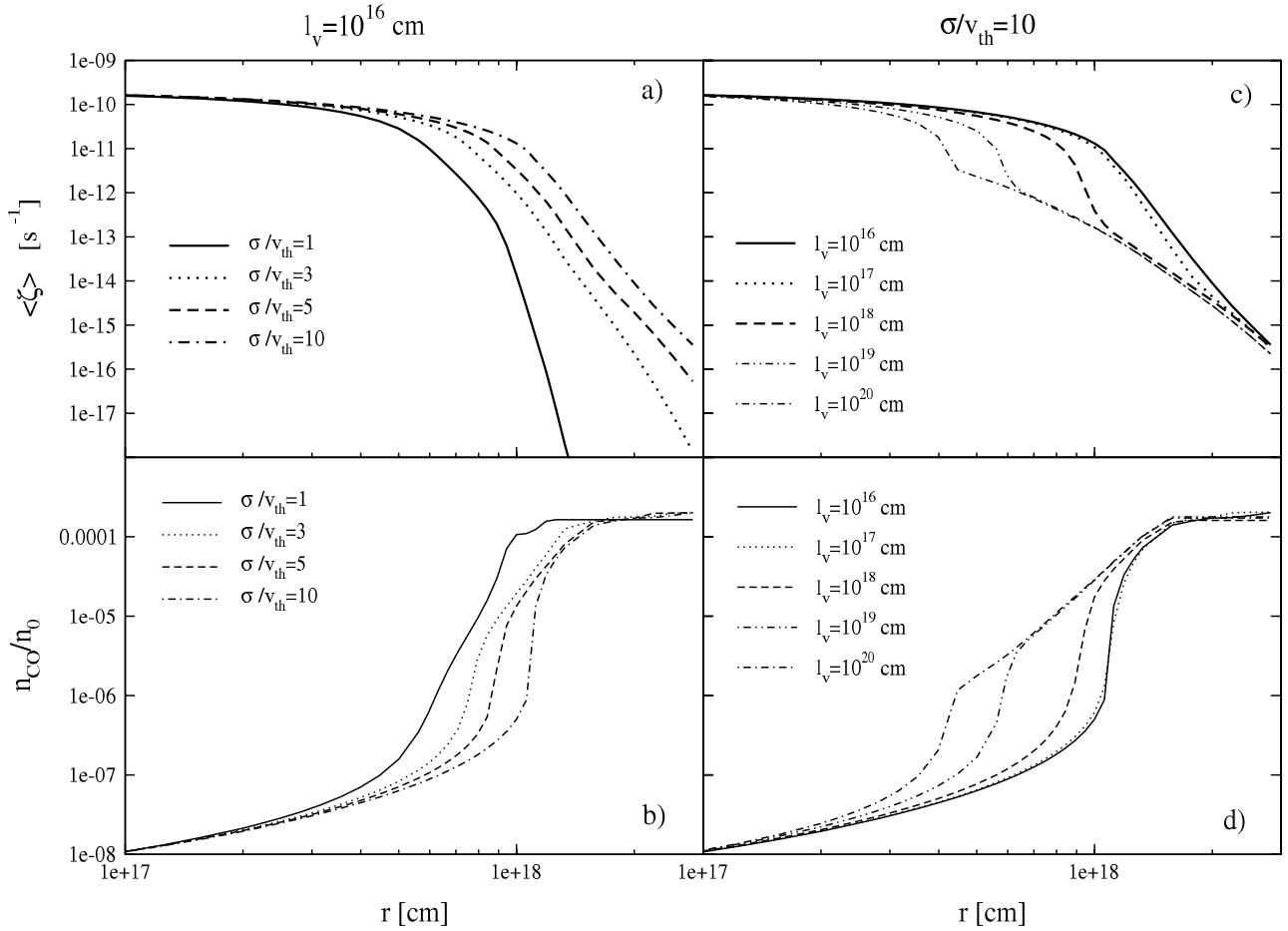

Fig. 3. Expectation values of the photodissociation rate coefficients $< \zeta >$ (*top*) and the corresponding relative CO abundance $< n_{\rm CO}/n >$ (*bottom*). **a)** and **b)** are for a correlation length of 10^{16} cm with different σ and **c)** and **d)** are for $\sigma/v_{\rm th} = 10$ and different correlation lengths. The density is $n = 1000$ cm^{-3} and $T = 15$ K.

2.8. Model parameters

We assume a simple plane-parallel geometry with uniform density $n = 500 \ldots 10\,000$ cm^{-3} and temperature $T = 15$, 50, 75 Kelvin. For the elemental abundances we adopted the values H:He:C:O = 1:0.1:3.6×10^{-4}:8.5×10^{-4}. The parameters of turbulence are varied between $\sigma/v_{\rm th} = 1 \ldots 10$ and $\ell = 10^{15} \ldots 10^{20}$ cm. The incident UV field is taken from Mezger et al. (1982) and is approximated by $4\pi J = 38.57 \lambda_{\mu{\rm m}}^{3.4172}$ erg cm^{-2} s^{-2} μm^{-1} with $912 \le \lambda \le 1118$ Å.

3. Results

In order to study the principal physical effects, and in order to save computing time we first investigated the influence of turbulence by modeling the absorption spectrum by one single line (compare with one line approximation by Spaans 1996). The resulting photodissociation rate coefficient was scaled to a rate coefficient at the cloud edge of $\sim 2 \times 10^{-10}$ s^{-1} in order to receive reasonable results from the chemical density calculations. Afterwards we accounted for the full absorption spectrum as described before and did calculations for a variety of different model parameters.

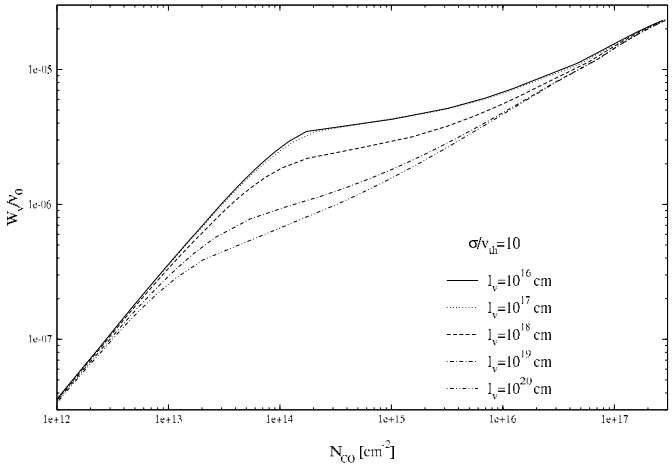

Fig. 4. Curves of growth for the single line approximation for different correlation legths and $\sigma/v_{\rm th} = 10$, $n = 1000$ cm^{-3}, $T = 15$ K.

3.1. Single line spectrum

In Fig. 4, curves of growth for different correlation lengths and a turbulent velocity of $\sigma/v_{\rm th} = 10$ for $n = 1000$ cm^{-3} and $T = 15$ K are shown. At high correlation lengths the line center becomes optically thick at much smaller CO column densities

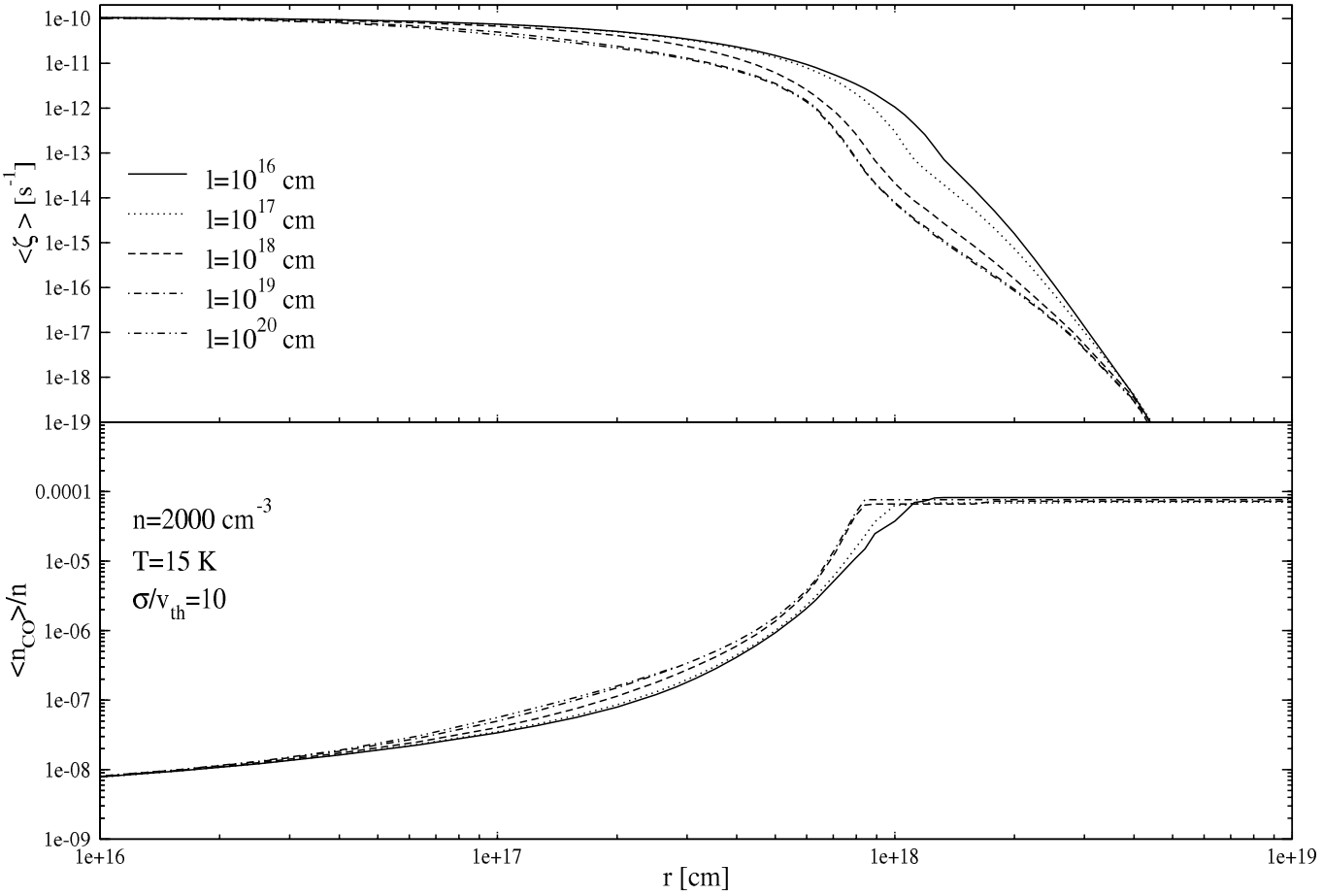

Fig. 5. Expectation values of photodissociation rate coefficients $< \zeta >$ (*top*) and corresponding relative CO abundance $< n_{\rm CO}/n >$ (*bottom*) in full spectral resolution. The density is $n = 2000$ cm^{-3}, $T = 15$ K and $\sigma/v_{\rm th} = 10$.

than is the case for smaller correlation length (compare e.g. Albrecht & Kegel). In Figs. 3c and d the corresponding expectation values of the photodissociation rate coefficients $< \zeta >$ (*top*) and the corresponding relative CO abundance $< n_{\rm CO}/n >$ (*bottom*) for the same models are shown. The penetration depth for photons decreases with increasing correlation length. The sharp bend in the curves for higher correlation lengths corresponds to the turning points in the curves of growth. In Figs. 3a and b, $< \zeta >$ and $< n_{\rm CO}/n >$ are plotted for a fixed (rather low) value of the correlation length and a set of different σ. Higher σ increase the photodissociation probability at a given cloud depth due to the stronger Doppler shift in different volume elements along the line of sight. Both effects, the influence of the correlation length ℓ and of the mean turbulent velocity σ, are well understood in principle but the quantitative influence is surprising, even in our crude model.

3.2. Full line spectrum

In the next step we accounted for a full absorption spectrum and did calculations for different model parameters. We determined the unshielded total photodissociation probability at the edge of the cloud. In contrast to earlier values of around 2×10^{-10} s^{-1} (e.g. van Dishoeck & Black 1988) we find a value of 1.02×10^{-10} s^{-1} which is comparable to results from Lee et al. (1996).

Figure 5 shows the depth dependent expectation values for the photodissociation probability and the relative CO density for calculations with the full line spectrum. We adopted a temperature of 15 K, $n = 2000$ cm^{-3}, and $\sigma/v_{\rm th} = 10$. As expected, the influence of a finite correlation length on the depth dependency is smaller than in the case of a single line absorption spectrum. The photodissociation now depends on a wide range of absorption bands that differently contribute to the total photodissociation probability at different cloud depths. Hence, the depth dependency is less strong than for a single absorption line. Nevertheless the influence is far from being negligible. Figure 6 shows the influence of mesoturbulence on the expectation value of the relative CO density for two different values of σ. The depth at which the CO density saturates is strongly dependent on the turbulence. For different correlations lengths and turbulent velocities the depth at which the CO density is no more influenced by the incident UV field differs by a factor of two. In the interpretation of observational data this difference may lead to an error in the estimation of the spatial cloud radius of up to 100%.

In order to compare the results of our calculations with commonly used methods, we plotted the expectation value of the photodissociation probability as well as the results from standard parametrized shielding factors as given by van Dishoeck & Black (1988) or Lee et al. (1996). Figure 7

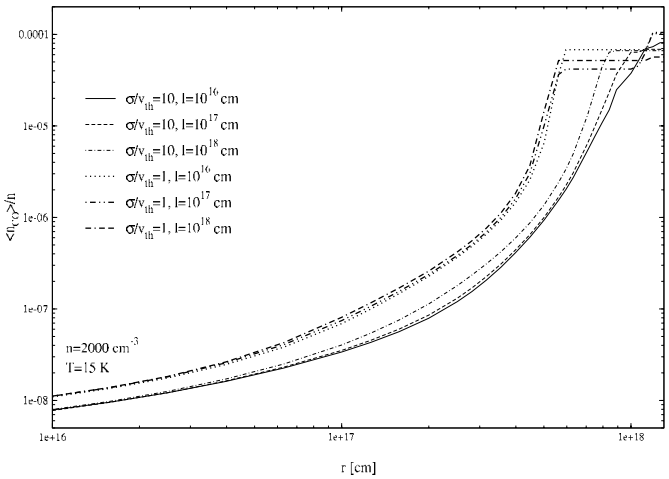

Fig. 6. Maximum model variations for the expected relative CO density due to mesoturbulent photodissociation of CO. The density is $n = 2000$ cm^{-3}, $T = 15$ K.

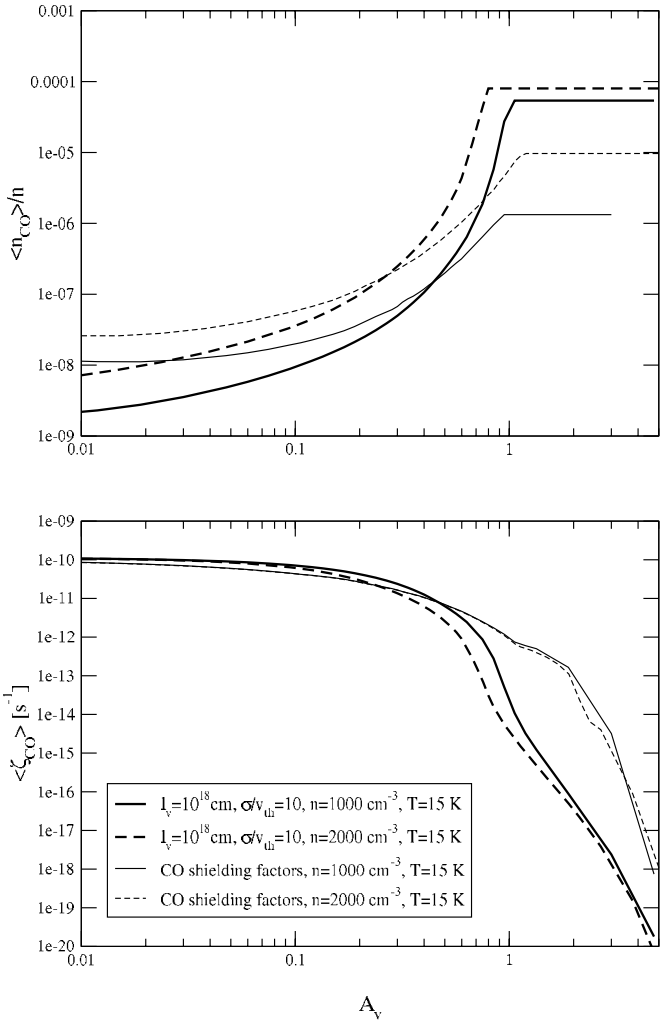

Fig. 7. Comparison of mesoturbulent calculations with standard shielding factors for two different cloud models. The unshielded photodissociation probability at the cloud edge is the same for both models ($\zeta_0 = 1 \times 10^{-10}$ s^{-1}). **Top:** expectation values for the relative CO density. **Bottom:** expectation values for the CO photodissociation probability.

shows this comparison for two different cloud models. The strong lines are results of our calculations and the thin lines are calculated from shielding factors. The difference in our results for different densities are due to the nonlinear coupling of the chemical rate equations with the radiative transfer and the varying ratio of correlation length to the mean free path of photons.

4. Discussion

We discussed the formation of CO molecules in interstellar molecular clouds under the influence of a UV radiation field. In particular we investigated the influence of a stochastic velocity distribution with finite correlation lengths on the photodissociation properties of CO molecules forming in interstellar clouds. At first the principle effects were studied by modeling the absorption spectrum by only one single line. The results show a strong dependency of the CO stratification on the turbulent velocity field in the cloud. In a second approach we accounted for the full UV absorption spectrum of CO. It turned out that the depth dependent properties of CO photodissociation and forming are affected. The results can be summarized as follows: a higher mean turbulent velocity of the stochastic velocity distribution along the line of sight leads to an increasing penetration depth of UV photons and therefore to a stronger photodissociation on CO molecules. On the other hand correlation length effects can lead to a decreasing photodissociation rate coefficient. By accounting for a finite correlation length of the mesoturbulent velocity field, the shielding of CO absorption bands is considerably enhanced and CO molecules can effectively form in depths that have a much stronger UV intensity in standard radiative transfer models. The depth dependent behavior of the photodissociation rate coefficient obtained from standard CO shielding factors show a large deviation from our results. This leads to significant differences in the interpretation of observational data. Therefore it may be neccessary to correct physical parameters of interstellar clouds derived by standard non-turbulent analysis.

Acknowledgements. This work was supported in part by the FAZIT Stiftung, Frankfurt a.M., Germany.

References

Albrecht, M. A., & Kegel, W. H. 1987, A&A, 176, 317
Boissé, P. 1990, A&A, 228, 483
Burke, J. R., & Hollenbach, D. J. 1983, ApJ, 265, 223
Eidelsberg, M., & Rostas, F. 1990, A&A, 235, 472
Eidelsberg, M., Benayoun, J. J., Viala, Y., & Rostas, F. 1991, A&AS, 90, 231
Eidelsberg, M., Benayoun, J. J., Viala, Y., et al. 1992, A&A, 265, 839
Falgarone, E., & Phillips, T. G. 1996, ApJ, 472, 191
Gail, H. P., Hundt, E., Kegel, W. H., Schmid–Burgk, J., & Traving, G. 1974, A&A, 32, 65

Gail, H.–P., Sedlmayr, E., & Traving, G. 1975, A&A, 44, 421
Gail, H. P., Sedlmayer, E., & Traving, G. 1979, J. Quant. Spectrosc. Radiat. Transf., 23, 267
Gail, H. P., & Sedlmayr, E. 1974, A&A, 36, 17
Hegmann, M., & Kegel, W. H. 1996, MNRAS, 283, 167
Hegmann, M., & Kegel, W. H. 2000, A&A, 359, 405
Hobson, M. P., & Scheuer, P. A. G. 1993, MNRAS, 264, 145
Hollenbach, D. J., & McKee, C. F. 1979, ApJ, 41, 555
Hollenbach, D. J., Takahashi, T., & Tielens, A. G. G. M. 1991, ApJ, 377, 192
Hollenbach, D. J., & Tielens, A. G. G. M. 1995, ARA&A, 35, 179
Kegel, W. H., Piehler, G., & Albrecht, M. A. 1993, A&A, 270, 407
Lee, H.-H., Herbst, E., Pineau Des Forets, G., Roueff, E., & Le Bourlot, J. 1996, A&A, 311, 690
Letzelter, C., Eidelsberg, M., Rostas, F., Breton, J., & Thieblemont, B. 1987, Chem. Phys., 114, 273
Le Teuff, Y. H., Millar, T. J., & Markwick, A. J. 2000, A&AS, 146, 157
Levshakov, S. A., & Kegel, W. H. 1994, MNRAS, 271, 161
Mezger, P. G., Mathis, J. S., & Panagia, N. 1982, A&A, 105, 372
Millar, T. J., Farquhar, P. R. A., & Willacy, K. 1995, A&AS, 121, 139
Piehler, G., & Kegel, W. H. 1995, A&A, 297, 841
Risken, H. 1988, The Fokker–Planck Equation (Berlin Heidelberg: Springer)
Roberge, W. G., Jones, D., Lepp, S., & Dalgarno, A. 1991, ApJS, 77, 287
Spaans, M. 1996, A&A, 307, 271
Spitzer, L. 1978, Physical Processes in the Interstellar Medium (New York: Wiley-Interscience)
Sternberg, A., & Dalgarno, A. 1995, ApJS, 99, 565
Tielens, A. G. G. M., & Hollenbach, D. 1985, ApJ, 291, 747
Tielens, A. G. G. M., & Hollenbach, D. 1985, ApJ, 291, 722
van Dishoeck, E. F., & Black, J. H. 1986, ApJS, 62, 109
van Dishoeck, E. F., & Black, J. H. 1988, ApJ, 334, 771
van Dishoeck, E. F., & Black, J. H. 1990, ApJ, 360, 314
Viala, Y. P., Letzelter, C., Eidelsberg, M., & Rostas, F. 1988, A&A, 193, 265
Warin, S., Benayoun, J. J., & Viala, Y. P. 1996, A&A, 308, 535